Intermolecular potential energy surface and thermophysical properties of propane

Robert Hellmann

Citation: The Journal of Chemical Physics **146**, 114304 (2017); doi: 10.1063/1.4978412
View online: http://dx.doi.org/10.1063/1.4978412
View Table of Contents: http://aip.scitation.org/toc/jcp/146/11
Published by the American Institute of Physics

Intermolecular potential energy surface and thermophysical properties of propane

Robert Hellmann[a)]
Institut für Chemie, Universität Rostock, 18059 Rostock, Germany

(Received 19 January 2017; accepted 27 February 2017; published online 16 March 2017)

A six-dimensional potential energy surface (PES) for the interaction of two rigid propane molecules was determined from supermolecular *ab initio* calculations up to the coupled cluster with single, double, and perturbative triple excitations level of theory for 9452 configurations. An analytical site-site potential function with 14 sites per molecule was fitted to the calculated interaction energies. To validate the analytical PES, the second virial coefficient and the dilute gas shear viscosity and thermal conductivity of propane were computed. The dispersion part of the potential function was slightly adjusted such that quantitative agreement with the most accurate experimental data for the second virial coefficient at room temperature was achieved. The adjusted PES yields values for the three properties that are in very good agreement with the best experimental data at all temperatures. *Published by AIP Publishing.* [http://dx.doi.org/10.1063/1.4978412]

I. INTRODUCTION

The calculation of the thermophysical properties of a fluid requires precise knowledge of the potential energy surface (PES) describing the interactions between the individual molecules. For dilute gases, the thermophysical properties are governed solely by binary interactions and therefore by the pair potentials, which can be determined with high accuracy for small molecules, see, for example, Refs. 1–6, using quantum-chemical *ab initio* methods. Provided that the pair potential functions are available, it is straightforward to calculate the second virial coefficient using statistical thermodynamics and the transport properties in the dilute gas limit using the kinetic theory of molecular gases.[7–9] At higher densities, it is important to account for nonadditive contributions to the interaction energy, at least at the three-body level, even for nonpolar and weakly polar substances.[10,11]

Propane (C_3H_8) is an important fluid with a wide range of practical applications. It is used as a fuel, a propellant, a refrigerant (R-290), and a chemical feedstock. Furthermore, it is utilized as a reference fluid in corresponding states approaches for the prediction of thermophysical properties. In all of these applications, there is a need for accurate thermophysical property values. However, most of the available experimental data for the thermodynamic and transport properties of propane are restricted to temperatures below 650 K.

Interactions between two propane molecules have been studied using high-level quantum-chemical *ab initio* methods by Gupta *et al.*,[12] by Tsuzuki *et al.*,[13–15] and by Jalkanen *et al.*,[16] but only Jalkanen *et al.*[16] fitted an analytical function to *ab initio* calculated interaction energies. Their site-site potential function was fitted to 1239 points on the PES obtained from supermolecular calculations using second-order Møller–Plesset perturbation theory (MP2) and a 6-311+G(2df,2pd) basis set.

In this work, we present a new pair potential for propane. It is based on supermolecular *ab initio* calculations up to the coupled cluster with single, double, and perturbative triple excitations [CCSD(T)][17] level of theory for 9452 points on the PES. A site-site potential function with 14 sites per molecule was fitted to the calculated interaction energies and validated by calculating the second virial coefficient and the dilute gas shear viscosity and thermal conductivity. The analytical potential function was further improved by performing an empirical adjustment using the most accurate experimental data for the second virial coefficient at room temperature as guidance. We also calculated the product of the molar density and the self-diffusion coefficient for the dilute gas limit, but there are no experimental data at low densities with which to compare. All thermophysical properties were computed for a large number of temperatures in the range from 150 K to 1200 K.

The paper is organized as follows. In Sec. II, we summarize the development of the new intermolecular potential function. In Sec. III, we present the computational details and results for the second virial coefficient and do the same for the transport properties in Sec. IV. A summary and conclusions are given in Sec. V.

II. INTERMOLECULAR POTENTIAL

A. Monomer geometry

The PES of two propane molecules is a 60-dimensional hypersurface if all inter- and intra-molecular degrees of freedom are considered. If both propane molecules are approximated as rigid rotors, the PES is only six-dimensional. Such an approach might be expected to be problematic at high temperatures due to the hindered rotations of the two methyl groups in each molecule, which have a torsional barrier of about 1660 K.[18] However, the average strength of the long-range attractive interactions and the "hard core volume" of each molecule, which are the features of the PES that mainly

a)Electronic mail: robert.hellmann@uni-rostock.de

determine the second virial coefficient and the transport properties, should not be significantly affected by the rotation of the methyl groups. Therefore, at least for the present application, the rigid-rotor approximation should be valid.

The monomer geometry was determined fully *ab initio* in several steps. First, a geometry optimization was performed at the all-electron CCSD(T) level of theory using the cc-pwCV5Z basis set[19] to obtain the best possible equilibrium geometry. Then, a geometry optimization was performed at the frozen-core CCSD(T)/cc-pVTZ[20] level, followed by a cubic force-field calculation at the same level of theory to obtain a zero-point vibrationally averaged geometry. Finally, the differences in the Cartesian coordinates of the atoms between the vibrationally averaged structure and the equilibrium structure at the frozen-core CCSD(T)/cc-pVTZ level were added to the Cartesian coordinates of the all-electron CCSD(T)/cc-pwCV5Z equilibrium structure. Thus, we obtained an approximation to the zero-point vibrationally averaged geometry at the all-electron CCSD(T)/cc-pwCV5Z level. The geometry is provided in the supplementary material.

B. *Ab initio* calculation of interaction energies

Each configuration of two rigid propane molecules can be expressed as a function of the distance R between the centers of mass of the two molecules and the five Euler angles $\theta_1, \psi_1, \theta_2, \psi_2$, and ϕ. Details concerning the precise definition of these angles can be found in the supplementary material. Two sets of angular configurations were generated by varying all five angles in steps of 45° starting at 0° and 22.5°, respectively, resulting in a total of 949 (405 + 544) distinct angular configurations. This is the same angular grid as in our study of the pair potential of ethylene oxide.[21] Twelve center-of-mass separations were considered for each angular configuration, with $2.0\,\text{Å} \leqslant R \leqslant 9.0\,\text{Å}$ for the first set of angles and $2.25\,\text{Å} \leqslant R \leqslant 10.0\,\text{Å}$ for the second one, resulting in 11 388 configurations. However, 1936 configurations with small values of R were discarded because of excessive overlap of the two molecules so that the final grid comprised 9452 configurations.

The interaction energies $V(R, \theta_1, \psi_1, \theta_2, \psi_2, \phi)$ were calculated employing the counterpoise-corrected supermolecular approach[22] at the frozen-core resolution of identity MP2 (RI-MP2)[23,24] level of theory with the RI-JK approximation[25,26] for the Hartree–Fock (HF) part. The aug-cc-pVXZ[27] basis sets with $X = 3$ (T) and $X = 4$ (Q) and corresponding cc-pVXZ-JKFIT[28] and aug-cc-pVXZ-MP2FIT[29] auxiliary basis sets were used for these calculations. We checked that, for a given value of X, the differences between the interaction energies obtained in this way and those obtained using the standard MP2 method are negligibly small. The correlation parts of the interaction energies, $V_{\text{RI-MP2 corr}}$, were extrapolated to the complete basis set (CBS) limit using the two-point scheme recommended by Halkier *et al.*,[30]

$$V_{\text{RI-MP2 corr}}(X) = V^{\text{CBS}}_{\text{RI-MP2 corr}} + \alpha X^{-3}. \tag{1}$$

The HF contributions were not extrapolated to the CBS limit because they are essentially converged at the $X = 4$ basis set level. For several configurations, we also performed calculations for $X = 5$ in order to compare RI-MP2/CBS interaction energies obtained using $X = 3$ and $X = 4$ with those obtained using $X = 4$ and $X = 5$. The differences are usually less than 0.1% and therefore negligible.

To further improve the accuracy of the interaction energies, we performed counterpoise-corrected supermolecular calculations also at the frozen-core CCSD(T)/aug-cc-pVDZ level for all 9452 configurations and added the differences between the CCSD(T)/aug-cc-pVDZ and MP2/aug-cc-pVDZ interaction energies to the RI-MP2/CBS ones. Thus, an approximation to the frozen-core CCSD(T)/CBS level was obtained. The CCSD(T) correction is mostly negative in the well region and mostly positive in the repulsive region. For about 80% of the configurations, it changes the interaction energy by less than 5%.

The results of the *ab initio* calculations for the 9452 investigated configurations of two propane molecules can be found in the supplementary material. The ORCA[31] and CFOUR[32] programs were used for all RI-MP2 and CCSD(T) calculations, respectively, reported in this work.

C. Analytical potential function

A site-site potential function with 14 sites per molecule was fitted to the calculated interaction energies. Each individual site-site interaction is represented as

$$V_{ij}(R_{ij}) = A_{ij}\exp(-\alpha_{ij}R_{ij}) - f_6(b_{ij}, R_{ij})\frac{C_{6\,ij}}{R_{ij}^6} - f_8(b_{ij}, R_{ij})\frac{C_{8\,ij}}{R_{ij}^8} + \frac{q_i q_j}{R_{ij}}, \tag{2}$$

where R_{ij} is the distance between site i in molecule 1 and site j in molecule 2. The damping functions f_n are given by[33]

$$f_n(b_{ij}, R_{ij}) = 1 - \exp(-b_{ij}R_{ij})\sum_{k=0}^{n}\frac{(b_{ij}R_{ij})^k}{k!}. \tag{3}$$

The total intermolecular potential is obtained as the sum of all site-site interactions,

$$V(R, \theta_1, \psi_1, \theta_2, \psi_2, \phi) = \sum_{i=1}^{14}\sum_{j=1}^{14} V_{ij}(R_{ij}). \tag{4}$$

Different basic arrangements of the 14 sites, consistent with the C_{2v} symmetry of propane, were tested. In the chosen arrangement, there are seven different types of sites, resulting in 28 different types of site-site combinations. The parameters A, α, b, C_6, and C_8 for these 28 combinations, the site charges q, and the Cartesian coordinates of the sites within the molecule were fully optimized in a non-linear least-squares fit to the 9452 calculated interaction energies using a weighting function w given by

$$w = \frac{\exp\left[0.005\left(R/\text{Å}\right)^3\right]}{\left[1 + 10^{-6}(V/\text{K} + 1000)^2\right]^2}. \tag{5}$$

The denominator of this function was chosen such that the weight of configurations increases with the interaction energy decreasing towards its global minimum ($V_{\text{min}} \approx -1000$ K), while the numerator ensures that the asymptotic region of the PES is adequately fitted. The site charges were constrained to

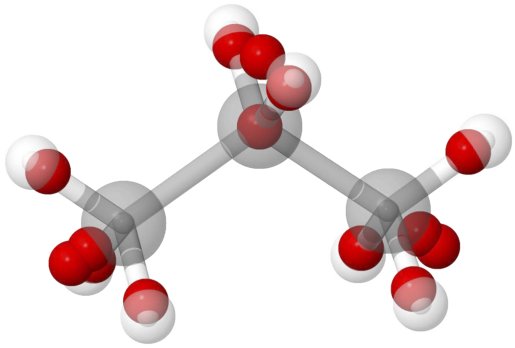

FIG. 1. Visualization of the optimized positions of the 14 interaction sites in the propane molecule.

yield neutral molecules with a dipole moment of 0.085 D. This value was obtained as a byproduct of the calculation of the equilibrium geometry at the all-electron CCSD(T)/cc-pwCV5Z level (see Sec. II A) and is close to the experimental value of 0.083 D.[34] The optimized positions of the 14 sites are visualized in Fig. 1.

In Fig. 2, the fitted interaction energies are plotted against the corresponding *ab initio* ones for energies up to 10 000 K. The mean absolute error (MAE) of the fit is 1.48 K for negative interaction energies, 15.7 K for positive ones up to 2000 K, and 95.1 K between 2000 K and 10 000 K. In the interval from 10 000 K to the highest interaction energies of about 180 000 K, the MAE increases even further. However, this region of the PES is of very little importance for the present application.

In our previous work on the CH_4–CH_4,[1] CH_4–N_2,[35] and CH_4–CO_2[36] PESs, we also employed zero-point vibrationally averaged monomer geometries and the highly accurate CCSD(T) method and extrapolated the interaction energies to the CBS limit. Nevertheless, the calculated values for the second virial coefficient of pure CH_4 and the CH_4–N_2 and CH_4–CO_2 cross second virial coefficients turned out to be systematically too positive in comparison with most experimental data sets. The main reason for the observed discrepancies is that using vibrationally averaged monomer geometries only partly accounts for vibrational effects on the interaction

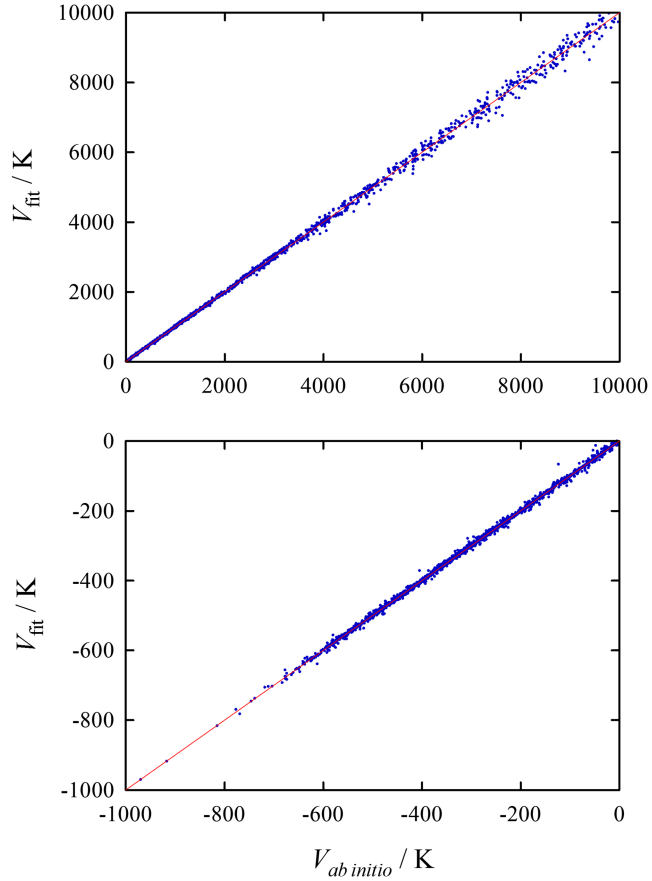

FIG. 2. Interaction energies from the fitted analytical potential function versus the *ab initio* calculated values. The red line is a guide to the eye corresponding to a perfect fit.

energies. Vibrations strongly increase the average polarizabilities of hydrocarbons and hence the strength of dispersion interactions involving hydrocarbons.[37–40] However, by adjusting a single dispersion-related parameter for each PES, we were able to bring the calculated values of the second virial coefficients into excellent agreement with the best experimental data at all temperatures.[1,35,36] In the present work, we have adjusted the fitted C_6 and C_8 parameters for the interactions

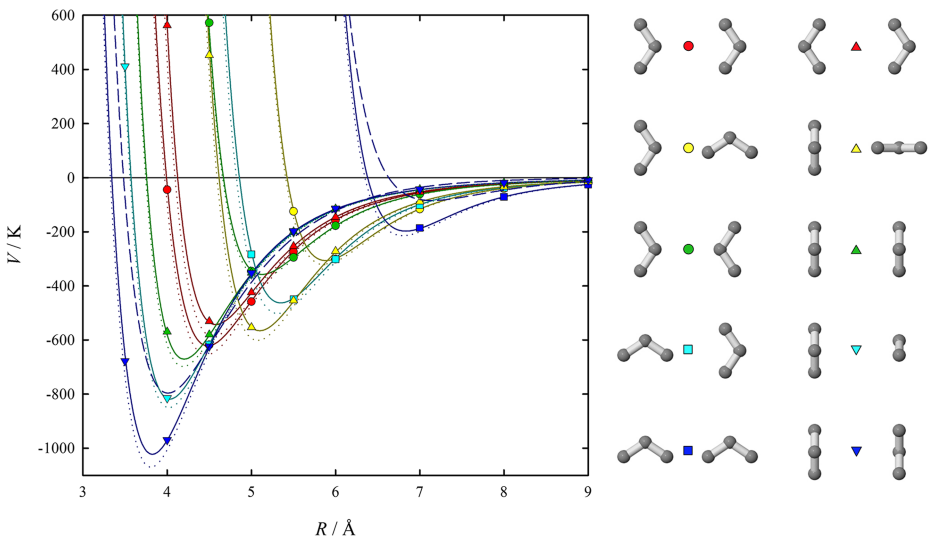

FIG. 3. Pair potential of two rigid propane molecules as a function of the center-of-mass distance R for 10 of the 949 investigated angular orientations (hydrogen atoms omitted for clarity). The *ab initio* calculated values are represented by symbols, the fitted potential function by solid lines, and the adjusted potential function by dotted lines. The dashed lines represent the PES of Jalkanen *et al.*[16] for the two orientations indicated by dark blue symbols.

of the three sites closest to the carbon atoms in molecule 1 with the respective three sites in molecule 2. Each of the C_6 parameters was changed by the same amount ΔC_6, while the C_8 parameters were adjusted by an amount ΔC_8 that was chosen such that the ratio of ΔC_8 and ΔC_6 is equal to the ratio of the isotropic averages of the total C_8 and C_6 dispersion coefficients of propane as determined by Thomas *et al.*[41] Thus, there is only a single adjustable parameter in this procedure. The best experimental data for the second virial coefficient at room temperature were used as reference for the adjustment, see Sec. III for details.

Figure 3 shows the distance dependence of the *ab initio* calculated interaction energies, of the fitted potential function, and of the adjusted potential function for 10 of the 949 investigated angular configurations. Furthermore, the distance dependence of the PES of Jalkanen *et al.*[16] is depicted for two of these orientations. It can be seen that the adjustment of the present PES does not significantly alter its qualitative features and that the PES of Jalkanen *et al.* is too repulsive in the well region, which is mainly due to the relatively small (by today's standards) 6-311+G(2df,2pd) basis set used.

The unadjusted potential function exhibits a total of 41 symmetry-distinct minima, whereas the adjusted one exhibits 40. All minimum structures and the corresponding interaction energies are listed in the supplementary material. A Fortran 90 routine computing the analytical potential function is also provided there.

III. SECOND VIRIAL COEFFICIENT

The classical second virial coefficient for a pure gas composed of rigid molecules is given by

$$B_2^{\mathrm{cl}}(T) = -\frac{1}{2}\int_0^\infty \langle f_{12}\rangle_{\Omega_1,\Omega_2} d\mathbf{R}, \tag{6}$$

where

$$f_{12} = \exp\left[-\frac{V(\mathbf{R},\Omega_1,\Omega_2)}{k_{\mathrm{B}}T}\right] - 1. \tag{7}$$

Here, T is the temperature, k_{B} is Boltzmann's constant, $\mathbf{R}$ is the distance vector between the centers of mass of the two molecules, Ω_1 and Ω_2 represent their angular orientations, and the angle brackets denote an average over Ω_1 and Ω_2. For molecules with masses and principal moments of inertia as large as in the case of propane, quantum effects can be accurately taken into account semiclassically by replacing the pair potential V in Eq. (7) by the quadratic Feynman–Hibbs (QFH) effective pair potential.[42] The QFH potential for two identical asymmetric-top molecules takes the form

$$V_{\mathrm{QFH}}(T) = V + \frac{\hbar^2}{12k_{\mathrm{B}}T}\left[\frac{1}{m}\left(\frac{\partial^2 V}{\partial x^2}+\frac{\partial^2 V}{\partial y^2}+\frac{\partial^2 V}{\partial z^2}\right) + \frac{1}{2}\sum_{n=1}^{2}\left(\frac{1}{I_a}\frac{\partial^2 V}{\partial \psi_{a,n}^2}+\frac{1}{I_b}\frac{\partial^2 V}{\partial \psi_{b,n}^2}+\frac{1}{I_c}\frac{\partial^2 V}{\partial \psi_{c,n}^2}\right)\right], \tag{8}$$

where m is the molecular mass; x, y, and z are the Cartesian components of $\mathbf{R}$; I_a, I_b, and I_c are the principal moments of inertia; and the angles $\psi_{a,n}$, $\psi_{b,n}$, and $\psi_{c,n}$ correspond to rotations of the nth molecule around its principal axes.

We calculated the second virial coefficient of propane at 121 temperatures in the range from 150 K to 1200 K, as well as at all temperatures for which experimental data are available, by means of the Mayer-sampling Monte Carlo (MSMC) method of Singh and Kofke.[43] The hard-sphere fluid with a sphere diameter of 6 Å was employed as reference system. Results were obtained simultaneously at all temperatures by performing multi-temperature simulations,[5,10,43] in

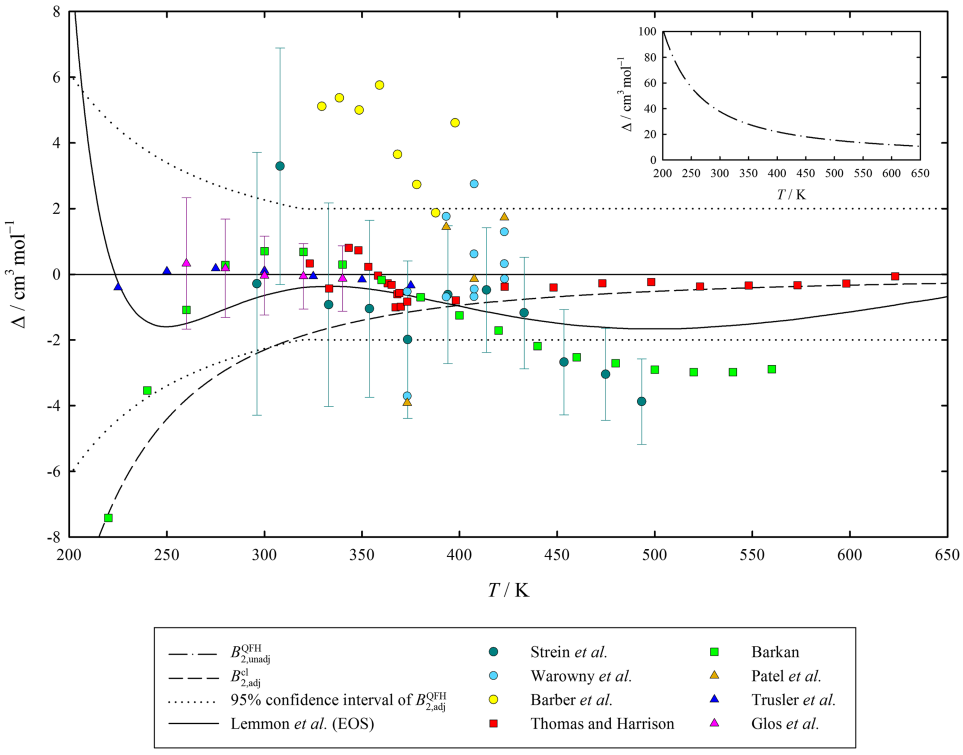

FIG. 4. Deviations, $\Delta = B_2 - B_{2,\mathrm{adj}}^{\mathrm{QFH}}$, of selected experimental data,[44–51] of values derived from the current reference EOS,[52] and of calculated values for the second virial coefficient of propane from values calculated semiclassically with the adjusted analytical potential function as a function of temperature.

which the absolute value of the integrand at 150 K was used as the sampling distribution. The second derivatives needed to compute the QFH potential [see Eq. (8)] were evaluated analytically. To avoid unphysical negative interaction energies at very small intermolecular separations R, the potential was set to infinity when R was smaller than 2 Å or when any of the site-site distances between the two molecules were smaller than 1.2 Å. In each MC step, one of the molecules was displaced and rotated, and the maximum step sizes for the moves were adjusted in short equilibration periods to achieve acceptance rates of 50%. Calculated virial coefficients from eight independent simulation runs of 2×10^{10} steps were averaged. The final results are converged to better than 0.15 $\mathrm{cm^3\ mol^{-1}}$ at all temperatures. They are listed for both the unadjusted and the adjusted potential in the supplementary material.

In Fig. 4, the values for the second virial coefficient calculated semiclassically using the adjusted potential function, $B_{2,\mathrm{adj}}^{\mathrm{QFH}}$, are compared with values calculated semiclassically using the unadjusted potential function, $B_{2,\mathrm{unadj}}^{\mathrm{QFH}}$, and classically using the adjusted one, $B_{2,\mathrm{adj}}^{\mathrm{cl}}$, as well as with selected experimental data[44–51] and values derived from the current reference equation of state (EOS) of Lemmon *et al.*[52] The experimental values of Trusler *et al.*[50] and of Glos *et al.*[51] at 300 K were used as reference for the adjustment of the analytical potential function described in Sec. II C, which lowers the calculated value of the second virial coefficient at this temperature from $-347.0\ \mathrm{cm^3\ mol^{-1}}$ to $-384.8\ \mathrm{cm^3\ mol^{-1}}$. The figure shows that the $B_{2,\mathrm{adj}}^{\mathrm{QFH}}$ values are in excellent agreement with all data points of Trusler *et al.*,[50] of Glos *et al.*,[51] and of Thomas and Harrison,[47] which together cover temperatures from 225 K to 623 K. This is remarkable considering the large differences between $B_{2,\mathrm{unadj}}^{\mathrm{QFH}}$ and $B_{2,\mathrm{adj}}^{\mathrm{QFH}}$.

Based on the comparison with the experimental data, a reasonable estimate of the combined expanded uncertainty U_c (95% confidence level) for $B_{2,\mathrm{adj}}^{\mathrm{QFH}}$ is

$$U_\mathrm{c}\left(B_{2,\mathrm{adj}}^{\mathrm{QFH}}\right) = \max\left[0.06\left(B_{2,\mathrm{unadj}}^{\mathrm{QFH}} - B_{2,\mathrm{adj}}^{\mathrm{QFH}}\right), 2\ \mathrm{cm^3\ mol^{-1}}\right], \tag{9}$$

which is also depicted in Fig. 4.

IV. TRANSPORT PROPERTIES

A. Theory and computational details

The transport properties in the dilute gas limit (i.e., the limit of zero density) can be calculated very efficiently using kinetic theory.[7–9] The shear viscosity η in this limit is given for a pure gas consisting of polyatomic molecules as

$$\eta = \frac{k_\mathrm{B}T}{\langle v\rangle}\frac{f_\eta^{(n)}}{\Im(2000)}, \tag{10}$$

where $\langle v\rangle = 4(k_\mathrm{B}T/\pi m)^{1/2}$ is the average relative thermal speed, $\Im(2000)$ is a temperature-dependent generalized cross section, and $f_\eta^{(n)}$ is an nth-order correction factor accounting for higher basis-function terms in the perturbation-series expansion of the solution of the Boltzmann equation.[7] Assuming that the vibrational states of the molecules do not change during collisions and that the vibrational motion of the molecules does not influence their trajectories, the thermal conductivity λ in the dilute gas limit can be written as a sum of a rigid-rotor contribution and a vibrational contribution,[53–55]

$$\lambda = \lambda_\mathrm{rr} + \lambda_\mathrm{vib}. \tag{11}$$

The rigid-rotor contribution is given as

$$\lambda_\mathrm{rr} = \frac{5k_\mathrm{B}^2T}{2m\langle v\rangle}\frac{S_{11}^{(1)} - rS_{21}^{(1)} - rS_{12}^{(1)} + r^2S_{22}^{(1)}}{S^{(1)}}f_{\lambda_\mathrm{rr}}^{(n)}, \tag{12}$$

where $S^{(1)}$ is a determinant of rigid-rotor cross sections,

$$S^{(1)} = \begin{vmatrix} \Im(1010)_\mathrm{rr} & \Im\begin{pmatrix}1010\\1001\end{pmatrix}_\mathrm{rr} \\ \Im\begin{pmatrix}1001\\1010\end{pmatrix}_\mathrm{rr} & \Im(1001)_\mathrm{rr} \end{vmatrix}, \tag{13}$$

and $S_{ij}^{(1)}$ are its minors. The dimensionless parameter r is given by

$$r = \left(\frac{2}{5}\frac{C_\mathrm{rot}}{k_\mathrm{B}}\right)^{1/2}, \tag{14}$$

where C_rot is the rotational contribution to the ideal gas heat capacity. The vibrational contribution to the thermal conductivity can be written as[53–55]

$$\lambda_\mathrm{vib} = N_\mathrm{A}C_\mathrm{vib}\rho_\mathrm{m}D_\mathrm{self}, \tag{15}$$

where N_A is Avogadro's constant, C_vib is the vibrational contribution to the ideal gas heat capacity, ρ_m is the molar density, and D_self is the self-diffusion coefficient. The product of the molar density and the self-diffusion coefficient in the dilute gas limit is given as

$$\rho_\mathrm{m}D_\mathrm{self} = \frac{k_\mathrm{B}T}{N_\mathrm{A}m\langle v\rangle}\frac{f_{D_\mathrm{self}}^{(n)}}{\sigma'(1000)}, \tag{16}$$

where $\sigma'(1000)$ denotes the so-called self-part of the cross section $\Im(1000)$.[55]

We computed the higher-order correction factors $f_\eta^{(n)}$, $f_{\lambda_\mathrm{rr}}^{(n)}$, and $f_{D_\mathrm{self}}^{(n)}$ up to $n=3$, $n=2$, and $n=2$, respectively, using expressions given in Refs. 6 and 55. Values of C_vib for propane were obtained from the formulation of the ideal gas heat capacity given by Lemmon *et al.*[52]

All generalized cross sections were calculated in the rigid-rotor approximation by means of the classical trajectory method using an extended version of the TRAJECT software code.[56,57] Classical trajectories describing collisions of two propane molecules were obtained by integrating Hamilton's equations for rigid asymmetric tops from pre-to post-collisional values. The initial and final separations were set to 500 Å. Total-energy-dependent generalized cross sections in the center-of-mass frame, which are 13-dimensional integrals over the initial states of the trajectories,[57] were calculated by means of a simple Monte Carlo procedure utilizing quasi-random numbers. The calculations were performed for 27 values of the total energy, $E = E_\mathrm{tr} + E_\mathrm{rot}$, divided into the three ranges $75\ \mathrm{K} \leqslant E \leqslant 500\ \mathrm{K}$, $500\ \mathrm{K} \leqslant E \leqslant 4000\ \mathrm{K}$, and $4000\ \mathrm{K} \leqslant E \leqslant 25\,000\ \mathrm{K}$. In each range, the energies were chosen as the pivot points for Chebyshev interpolation of the cross sections as a function of $\ln(E)$. Up to 2×10^6 trajectories were computed at each total energy value. For $E < 500$ K, the

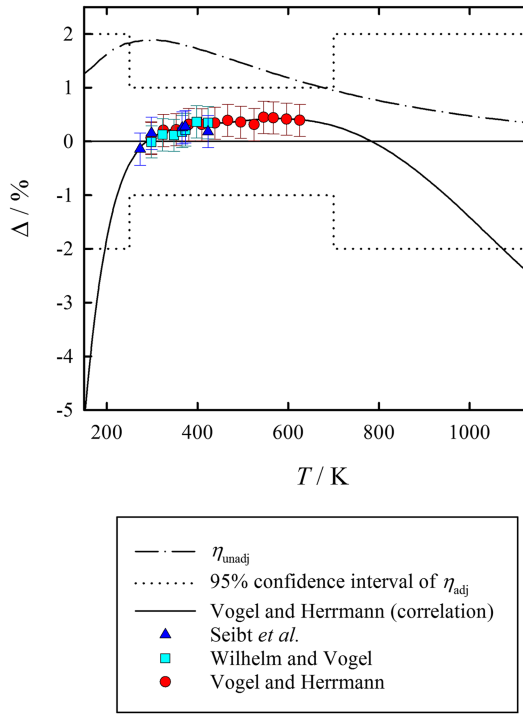

FIG. 5. Relative deviations, $\Delta = (\eta - \eta_{adj})/\eta_{adj}$, of selected experimental data,[60–62] of a correlation,[62] and of calculated values for the shear viscosity of dilute propane from values calculated using the adjusted analytical potential function as a function of temperature.

number of trajectories had to be reduced because the computational demand required to calculate a trajectory with sufficient accuracy increases with decreasing energy. For example, only 200 000 trajectories were calculated at E = 75 K. However, the contributions of such low energies to the transport properties at temperatures above 150 K are negligibly small. An integration over E yielded temperature-dependent generalized cross sections in the center-of-mass frame.[57] Finally, the center-of-mass cross sections were converted to laboratory frame cross sections.[57,58]

B. Results

The higher-order correction factors $f_\eta^{(3)}$, $f_{\lambda_{rr}}^{(2)}$, and $f_{D_{self}}^{(2)}$ and the ratio $f_\eta^{(3)}/f_\eta^{(2)}$ differ from unity by at most +0.8%, +1.7%, +0.3%, and +0.03%, respectively, which is in line with the respective values obtained for other molecular gases.[8,59] As expected, the vibrational contribution to the thermal conductivity, λ_{vib}, increases rapidly with temperature. It amounts to 31.3%, 56.3%, and 82.8% of the total thermal conductivity λ at 150 K, 300 K, and 1200 K, respectively.

Calculated values of the dilute gas transport properties at 96 temperatures in the range from 150 K to 1200 K are listed for both the unadjusted and the adjusted potential in the supplementary material. The relative standard uncertainties of these values due to the Monte Carlo integration over the initial states of the trajectories are smaller than 0.15% for viscosity and self-diffusion and 0.3% for thermal conductivity at all temperatures. The uncertainties due to the numerical integration of Hamilton's equations and due to the limited number of energy pivot points are negligible.

In Fig. 5, the viscosity values obtained using the adjusted potential function, η_{adj}, are compared with those obtained using the unadjusted one, η_{unadj}, with the experimental data reported by Seibt *et al.*,[60] by Wilhelm and Vogel,[61] and by Vogel and Herrmann,[62] as well as with the zero-density part of the correlation of Vogel and Herrmann.[62] According to the assessment of Vogel and Herrmann,[62] the three selected data

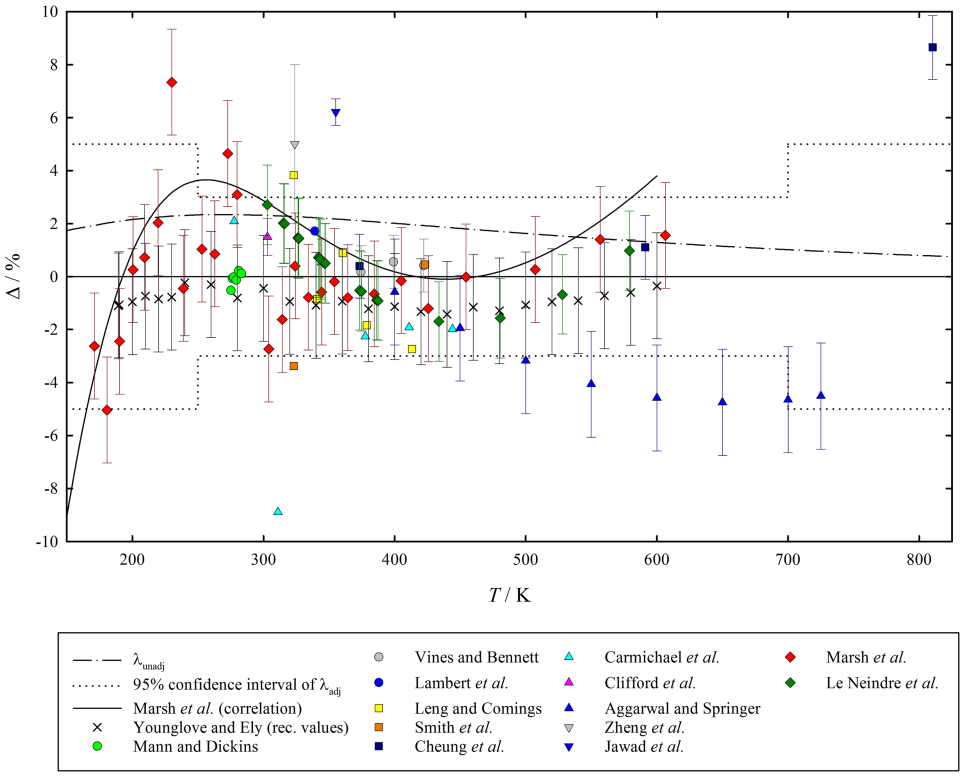

FIG. 6. Relative deviations, $\Delta = (\lambda - \lambda_{adj})/\lambda_{adj}$, of selected experimental data,[63–75] of a correlation,[74] of recommended reference values,[76] and of calculated values for the thermal conductivity of dilute propane from values calculated using the adjusted analytical potential function as a function of temperature.

sets are the most accurate to date for propane in the dilute gas phase with an uncertainty of only 0.3%. They are mutually consistent and extend over the whole range of temperatures at which experimental data for the gas phase are available (273 K to 625 K). Thus, there is no need to include further data sets in the comparison. The figure shows that the agreement of the η_{adj} values with the three data sets is essentially perfect around room temperature. At higher temperatures, the deviations from η_{adj} increase to about +0.4%. The correlation of Vogel and Herrmann[62] fits the three experimental data sets perfectly but deviates from η_{adj} by −5.2% at 150 K and −2.9% at 1200 K. However, the correlation is valid only up to 650 K and has an expanded uncertainty (95% confidence level) of 6% below 273 K. Viscosity values obtained with the unadjusted potential, η_{unadj}, deviate by +1.9% from η_{adj} around room temperature, although the deviations decrease towards both lower and higher temperatures.

Based on the comparison with the experimental data, the relative combined expanded uncertainty (95% confidence level) for η_{adj} is estimated to be 1% between 250 K and 700 K, increasing to 2% below 250 K and above 700 K. The uncertainty estimate is also depicted in Fig. 5.

In Fig. 6, the thermal conductivity values obtained using the adjusted potential function, λ_{adj}, are compared with those obtained using the unadjusted one, λ_{unadj}, with a large number of experimental data sets,[63–75] with the zero-density part of the correlation of Marsh *et al.*,[74] and with the recommended reference values of Younglove and Ely.[76] We extrapolated the data of Zheng *et al.*[72] at 323.75 K and the steady-state hot-wire data of Marsh *et al.*[74] to zero pressure. The transient hot-wire data of Marsh *et al.* from the same paper[74] are not included in the comparison because these authors found them to be affected by large systematic errors in the dilute gas phase. For all other data sets shown in Fig. 6, we used the values from the original papers for the zero-density limit or, where such values were not provided, for the lowest pressure. The figure shows that most of the experimental data and the recommended values of Younglove and Ely agree remarkably well with λ_{adj}, but deviate systematically from λ_{unadj}, which differs from λ_{adj} in a similar manner as η_{unadj} from η_{adj}.

The relative combined expanded uncertainty (95% confidence level) for λ_{adj} is estimated to be 3% between 250 K and 700 K, increasing to 5% below 250 K and above 700 K. This estimate is not only based on the comparison with the experimental data but also takes into account that the approximations involved in the kinetic theory approach used in this work affect the thermal conductivity more significantly than the other transport properties. The uncertainty estimate is also depicted in Fig. 6.

There are no experimental data for the self-diffusion coefficient of dilute propane with which to compare. The relative combined expanded uncertainty (95% confidence level) for $\rho_m D_{self}$ is conservatively estimated to be 2% between 250 K and 700 K, increasing to 3% below 250 K and above 700 K.

V. SUMMARY AND CONCLUSIONS

A new six-dimensional intermolecular PES for two rigid propane molecules has been developed. It is based on counterpoise-corrected supermolecular *ab initio* calculations at the RI-MP2/aug-cc-pVTZ and RI-MP2/aug-cc-pVQZ levels of theory for 9452 configurations. The calculated interaction energies were extrapolated to the CBS limit and further improved by adding a correction for the higher CCSD(T) level of theory computed using the aug-cc-pVDZ basis set. A site-site potential function with 14 sites per molecule and isotropic site-site interactions was fitted to the calculated interaction energies. In order to properly account for zero-point vibrational effects, the potential function was adjusted in a physically reasonable manner to reproduce the most accurate experimental data for the second virial coefficient at room temperature.

The new PES was validated by computing the second virial coefficient and the dilute gas shear viscosity and thermal conductivity. For all three properties, the comparison with the best available experimental data showed remarkably good agreement at all temperatures for the adjusted PES and large systematic deviations for the unadjusted one, thus demonstrating the appropriateness of the adjustment procedure. Furthermore, it can be concluded that the presence of methyl groups, which can undergo a hindered rotation, does not significantly affect the accuracy of the rigid-rotor approximation for the calculation of the second virial coefficient and the dilute gas transport properties. The product of molar density and self-diffusion coefficient in the dilute gas limit was also computed, but there are no experimental data to compare with. Calculated values for all thermophysical properties are provided at temperatures from 150 K to 1200 K in the supplementary material. They can be used to supplement the best experimental data in the development of advanced reference correlations. A recent example of such an approach is the new reference correlation for the thermal conductivity of carbon dioxide.[77]

SUPPLEMENTARY MATERIAL

See supplementary material for the monomer geometry, details of the Euler angles used, results of the *ab initio* calculations for all 9452 investigated configurations of two propane molecules, a Fortran 90 routine computing the analytical potential function, a list of the minimum structures, and tables of calculated values for the second virial coefficient and the dilute gas transport properties.

ACKNOWLEDGMENTS

The author thanks Benjamin Jäger for the calculation and analysis of the vibrationally averaged propane geometry. This work was financially supported by the Deutsche Forschungsgemeinschaft (DFG), Grant No. HE 6155/2-1.

[1] R. Hellmann, E. Bich, and E. Vogel, J. Chem. Phys. **128**, 214303 (2008).
[2] R. Bukowski, K. Szalewicz, G. C. Groenenboom, and A. van der Avoird, J. Chem. Phys. **128**, 094314 (2008).
[3] R. J. Wheatley and A. H. Harvey, J. Chem. Phys. **134**, 134309 (2011).
[4] R. Hellmann, E. Bich, E. Vogel, and V. Vesovic, Phys. Chem. Chem. Phys. **13**, 13749 (2011).
[5] R. Hellmann, Mol. Phys. **111**, 387 (2013).
[6] R. Hellmann, Chem. Phys. Lett. **613**, 133 (2014).
[7] F. R. W. McCourt, J. J. M. Beenakker, W. E. Köhler, and I. Kuščer, *Nonequilibrium Phenomena in Polyatomic Gases, Vol. I: Dilute Gases* (Clarendon Press, Oxford, 1990).

[8] E. Bich, J. B. Mehl, R. Hellmann, and V. Vesovic, in *Experimental Thermodynamics Volume IX: Advances in Transport Properties of Fluids*, edited by M. J. Assael, A. R. H. Goodwin, V. Vesovic, and W. A. Wakeham (The Royal Society of Chemistry, Cambridge, 2014), Chap. 7, pp. 226–252.
[9] R. Hellmann, E. Bich, and V. Vesovic, J. Chem. Phys. **144**, 134301 (2016).
[10] B. Jäger, R. Hellmann, E. Bich, and E. Vogel, J. Chem. Phys. **135**, 084308 (2011).
[11] R. Hellmann, J. Chem. Phys. **146**, 054302 (2017).
[12] S. Gupta, J. Yang, and N. R. Kestner, J. Chem. Phys. **89**, 3733 (1988).
[13] S. Tsuzuki, T. Uchimaru, M. Mikami, and K. Tanabe, J. Phys. Chem. A **102**, 2091 (1998).
[14] S. Tsuzuki, T. Uchimaru, M. Mikami, and K. Tanabe, J. Phys. Chem. A **106**, 3867 (2002).
[15] S. Tsuzuki, K. Honda, T. Uchimaru, and M. Mikami, J. Chem. Phys. **124**, 114304 (2006).
[16] J.-P. Jalkanen, R. Mahlanen, T. A. Pakkanen, and R. L. Rowley, J. Chem. Phys. **116**, 1303 (2002).
[17] K. Raghavachari, G. W. Trucks, J. A. Pople, and M. Head-Gordon, Chem. Phys. Lett. **157**, 479 (1989).
[18] J. Chao, R. C. Wilhoit, and B. J. Zwolinski, J. Phys. Chem. Ref. Data **2**, 427 (1973).
[19] K. A. Peterson and T. H. Dunning, Jr., J. Chem. Phys. **117**, 10548 (2002).
[20] T. H. Dunning, Jr., J. Chem. Phys. **90**, 1007 (1989).
[21] J.-P. Crusius, R. Hellmann, E. Hassel, and E. Bich, J. Chem. Phys. **141**, 164322 (2014).
[22] S. F. Boys and F. Bernardi, Mol. Phys. **19**, 553 (1970).
[23] F. Weigend and M. Häser, Theor. Chem. Acc. **97**, 331 (1997).
[24] F. Weigend, M. Häser, H. Patzelt, and R. Ahlrichs, Chem. Phys. Lett. **294**, 143 (1998).
[25] F. Weigend, M. Kattannek, and R. Ahlrichs, J. Chem. Phys. **130**, 164106 (2009).
[26] S. Kossmann and F. Neese, Chem. Phys. Lett. **481**, 240 (2009).
[27] R. A. Kendall, T. H. Dunning, Jr., and R. J. Harrison, J. Chem. Phys. **96**, 6796 (1992).
[28] F. Weigend, Phys. Chem. Chem. Phys. **4**, 4285 (2002).
[29] F. Weigend, A. Köhn, and C. Hättig, J. Chem. Phys. **116**, 3175 (2002).
[30] A. Halkier, T. Helgaker, P. Jørgensen, W. Klopper, H. Koch, J. Olsen, and A. K. Wilson, Chem. Phys. Lett. **286**, 243 (1998).
[31] F. Neese, Wiley Interdiscip. Rev.: Comput. Mol. Sci. **2**, 73 (2012).
[32] CFOUR, Coupled-Cluster techniques for Computational Chemistry, a quantum-chemical program package by J. F. Stanton, J. Gauss, M. E. Harding, P. G. Szalay with contributions from A. A. Auer, R. J. Bartlett, U. Benedikt, C. Berger, D. E. Bernholdt, Y. J. Bomble, L. Cheng, O. Christiansen, M. Heckert, O. Heun, C. Huber, T.-C. Jagau, D. Jonsson, J. Jusélius, K. Klein, W. J. Lauderdale, D. A. Matthews, T. Metzroth, L. A. Mück, D. P. O'Neill, D. R. Price, E. Prochnow, C. Puzzarini, K. Ruud, F. Schiffmann, W. Schwalbach, S. Stopkowicz, A. Tajti, J. Vázquez, F. Wang, J. D. Watts and the integral packages MOLECULE (J. Almlöf and P. R. Taylor), PROPS (P. R. Taylor), ABACUS (T. Helgaker, H. J. Aa. Jensen, P. Jørgensen, and J. Olsen), and ECP routines by A. V. Mitin and C. van Wüllen. For the current version, see http://www.cfour.de.
[33] K. T. Tang and J. P. Toennies, J. Chem. Phys. **80**, 3726 (1984).
[34] D. R. Lide, Jr., J. Chem. Phys. **33**, 1514 (1960).
[35] R. Hellmann, E. Bich, E. Vogel, and V. Vesovic, J. Chem. Phys. **141**, 224301 (2014).
[36] R. Hellmann, E. Bich, and V. Vesovic, J. Chem. Thermodyn. **102**, 429 (2016).
[37] A. J. Russell and M. A. Spackman, Mol. Phys. **84**, 1239 (1995).
[38] D. M. Bishop, F. L. Gu, and S. M. Cybulski, J. Chem. Phys. **109**, 8407 (1998).
[39] A. J. Russell and M. A. Spackman, Mol. Phys. **98**, 867 (2000).
[40] S. M. Cybulski and T. P. Haley, J. Chem. Phys. **121**, 7711 (2004).
[41] G. F. Thomas, F. Mulder, and W. J. Meath, Chem. Phys. **54**, 45 (1980).
[42] R. P. Feynman and A. R. Hibbs, *Quantum Mechanics and Path Integrals* (McGraw-Hill, New York, 1965).
[43] J. K. Singh and D. A. Kofke, Phys. Rev. Lett. **92**, 220601 (2004).
[44] K. Strein, R. N. Lichtenthaler, B. Schramm, and K. Schäfer, Ber. Bunsenges. Phys. Chem. **75**, 1308 (1971).
[45] W. Warowny, P. Wielopolski, and J. Stecki, Phys. A **91**, 73 (1978).
[46] J. R. Barber, W. B. Kay, and A. S. Teja, AIChE J. **28**, 142 (1982).
[47] R. H. P. Thomas and R. H. Harrison, J. Chem. Eng. Data **27**, 1 (1982).
[48] E. S. Barkan, Russ. J. Phys. Chem. **57**, 1351 (1983).
[49] M. R. Patel, L. L. Joffrion, and P. T. Eubank, AIChE J. **34**, 1229 (1988).
[50] J. P. M. Trusler, W. A. Wakeham, and M. P. Zarari, Int. J. Thermophys. **17**, 35 (1996).
[51] S. Glos, R. Kleinrahm, and W. Wagner, J. Chem. Thermodyn. **36**, 1037 (2004).
[52] E. W. Lemmon, M. O. McLinden, and W. Wagner, J. Chem. Eng. Data **54**, 3141 (2009).
[53] Z. Liang and H.-L. Tsai, Fluid Phase Equilib. **297**, 40 (2010).
[54] Z. Liang and H.-L. Tsai, Mol. Phys. **108**, 1707 (2010).
[55] R. Hellmann and E. Bich, Mol. Phys. **113**, 176 (2015).
[56] E. L. Heck and A. S. Dickinson, Comput. Phys. Commun. **95**, 190 (1996).
[57] A. S. Dickinson, R. Hellmann, E. Bich, and E. Vogel, Phys. Chem. Chem. Phys. **9**, 2836 (2007).
[58] C. F. Curtiss, J. Chem. Phys. **75**, 1341 (1981).
[59] R. Hellmann and E. Bich, Mol. Phys. (published online).
[60] D. Seibt, K. Voß, S. Herrmann, E. Vogel, and E. Hassel, J. Chem. Eng. Data **56**, 1476 (2011).
[61] J. Wilhelm and E. Vogel, J. Chem. Eng. Data **56**, 1722 (2011).
[62] E. Vogel and S. Herrmann, J. Phys. Chem. Ref. Data **45**, 043103 (2016).
[63] W. B. Mann and B. G. Dickins, Proc. R. Soc. London, Ser. A **134**, 77 (1931).
[64] R. G. Vines and L. A. Bennett, J. Chem. Phys. **22**, 360 (1954).
[65] J. D. Lambert, K. J. Cotton, M. W. Pailthorpe, A. M. Robinson, J. Scrivins, W. R. F. Vale, and R. M. Young, Proc. R. Soc. London, Ser. A **231**, 280 (1955).
[66] D. E. Leng and E. W. Comings, Ind. Eng. Chem. **49**, 2042 (1957).
[67] W. J. S. Smith, L. D. Durbin, and R. Kobayashi, J. Chem. Eng. Data **5**, 316 (1960).
[68] H. Cheung, L. A. Bromley, and C. R. Wilke, AIChE J. **8**, 221 (1962).
[69] L. T. Carmichael, J. Jacobs, and B. H. Sage, J. Chem. Eng. Data **13**, 40 (1968).
[70] A. A. Clifford, E. Dickinson, and P. Gray, J. Chem. Soc., Faraday Trans. 1 **72**, 1997 (1976).
[71] M. C. Aggarwal and G. S. Springer, J. Chem. Phys. **70**, 3948 (1979).
[72] X.-Y. Zheng, S. Yamamoto, H. Yoshida, H. Masuoka, and M. Yorizane, J. Chem. Eng. Jpn. **17**, 237 (1984).
[73] S. H. Jawad, M. J. Dix, and W. A. Wakeham, Int. J. Thermophys. **20**, 45 (1999).
[74] K. N. Marsh, R. A. Perkins, and M. L. V. Ramires, J. Chem. Eng. Data **47**, 932 (2002).
[75] B. Le Neindre, Y. Garrabos, and M. Nikravech, J. Chem. Eng. Data **59**, 3422 (2014).
[76] B. A. Younglove and J. F. Ely, J. Phys. Chem. Ref. Data **16**, 577 (1987).
[77] M. L. Huber, E. A. Sykioti, M. J. Assael, and R. A. Perkins, J. Phys. Chem. Ref. Data **45**, 013102 (2016).